

**Molecular Cell, Volume 84**

**Supplemental information**

**Recruitment of trimeric eIF2 by phosphatase**

**non-catalytic subunit PPP1R15B**

**Agnieszka Fatajska, George Hodgson, Stefan M.V. Freund, Sarah L. Maslen, Tomos Morgan, Sigurdur R. Thorkelsson, Marjon van Slegtenhorst, Sonja Lorenz, Antonina Andreeva, Laura Donker Kaat, and Anne Bertolotti**

**Molecular Cell, Volume 84**

**Supplemental information**

**Recruitment of trimeric eIF2 by phosphatase**

**non-catalytic subunit PPP1R15B**

**Agnieszka Fatajska, George Hodgson, Stefan M.V. Freund, Sarah L. Maslen, Tomos Morgan, Sigurdur R. Thorkelsson, Marjon van Slegtenhorst, Sonja Lorenz, Antonina Andreeva, Laura Donker Kaat, and Anne Bertolotti**

## Supplemental information

Figures S1-S6 and accompanying text

Table S2

### **Figure S1 Multiple sequence alignment of R15B orthologs. Related to Figure 1**

Sequences were aligned using Mafft<sup>76</sup> and coloured according to Clustal<sup>80</sup> colouring scheme. Colour intensity indicates sequence conservation. A black arrow shows the beginning of the fragment used in this study.

### **Figure S2 HDX-MS analyses of eIF2 in the presence of R15B<sup>414-613</sup>. Related to Figure 2**

(A-C) Sequence coverage map in HDX-MS analyses of eIF2 $\alpha$  (A),  $\beta$  (B) and  $\gamma$  (C) in presence of R15B<sup>414-613</sup>. Bars represent the peptic peptides of eIF2 plotted against the amino acid sequence.

(D-L) Woods plots showing differences in deuterium uptake for eIF2 in the presence or absence of R15B<sup>414-613</sup>. Deprotected, protected and non-significantly different peptides are in red, blue and grey respectively plotted as  $\Delta$  fraction exchanged (Y-axis). Bar length corresponds to peptide length plotted against the sequence position (X-axis). Dashed and dotted lines indicate 98 and 99% confidence intervals applied to identify peptides with statistically significant deuteration differences. Data for eIF2 $\alpha$  3 sec, 30 sec, 50 min; eIF2 $\beta$  30 sec, 5 min, 50 min and eIF2 $\gamma$  30 sec, 5 min and 50 min are shown in panels (D-L) respectively. Error bars denote combined uncertainty of peptide deuteration calculated based on triplicate experiments.

### **Figure S3 HDX-MS analyses for R15B<sup>414-613</sup>. Related to Figure 3**

(A) Plot showing HDX for a given R15B<sup>414-613</sup> peptide following 3 sec incubation with D<sub>2</sub>O. Bars indicate the peptic peptides of R15B<sup>414-613</sup> plotted against the amino acid sequence (X-axis). Y-axis: fraction of deuteration peptide compared to maximum level of measured deuteration. Error bars represent combined uncertainty calculated on triplicate experiments.

(B) Sequence coverage of R15B<sup>414-613</sup> in presence of eIF2 in HDX analyses. Bars indicate the peptic peptides of R15B<sup>414-613</sup> plotted on the amino acid sequence.

**Figure S4  $^{15}\text{N}$  backbone relaxation of R15B<sup>414-613</sup> alone and in the presence of 10% eIF2. Related to Figure 4.**

(A-E) Experimental  $^{15}\text{N}$  backbone relaxation data for R15B<sup>414-613</sup> at 281.5K.

(G-K) Experimental  $^{15}\text{N}$  backbone relaxation data for R15B<sup>414-613</sup> in the presence of eIF2 at 281.5K.

(A, G)  $\{^1\text{H}\}$ - $^{15}\text{N}$  NOE,

(B, H)  $R_2$

(C, I)  $\eta_{xy}$

(D, J)  $R_1$

(E, K) Superposition of measured  $R_2$  (black line) and calculated exchange free  $R_2^0$  (blue). Exchange contribution ( $R_{ex}$ , red line).

(F) Peak intensity ratio of  $^1\text{H}$ ,  $^{15}\text{N}$  2D spectra of R15B<sup>414-613</sup> on its own and after addition of 10% eIF2, only a modest degree of local attenuation was observed.

**Figure S5 Sequence alignments of R15B<sup>414-639</sup>. Related to Figure 5**

(A) Pair-wise sequence alignments of the human R15B sequence repeats.

(B) Multiple sequence alignments of the first R15B repeat and the homologous sequence repeats identified in human R15A.

(C) Same as in (B) with the addition of R15 from *Drosophila melanogaster* (dm), ICP34 from the human Herpes simplex virus 1 (hhv1) and DP71L from the African swine fever virus (asfv).

**Figure S6 pLDDT of R15B-eIF2 AlphaFold2 model. Related to Figure 7**

(A) pLDDT scores shown for R15B<sup>414-613</sup>, eIF2 $\alpha$  1-315, eIF2 $\beta$  167-333, eIF2 $\gamma$  1-472 as a contiguous representation.

(B) As in (A) with R15B<sup>414-500</sup>.

**Table S2 Oligonucleotides used in this study. Related to STAR methods.**



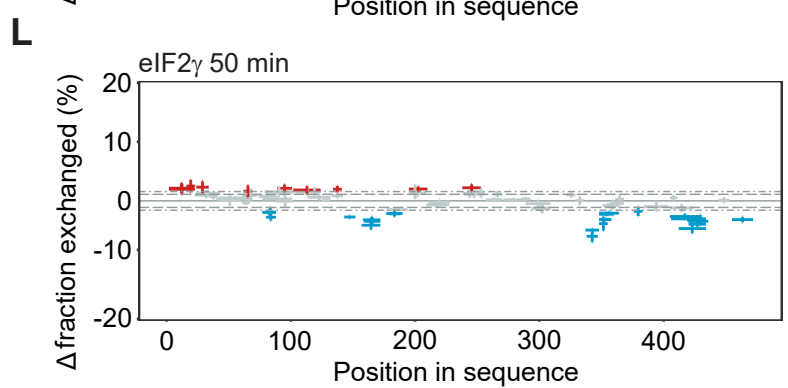
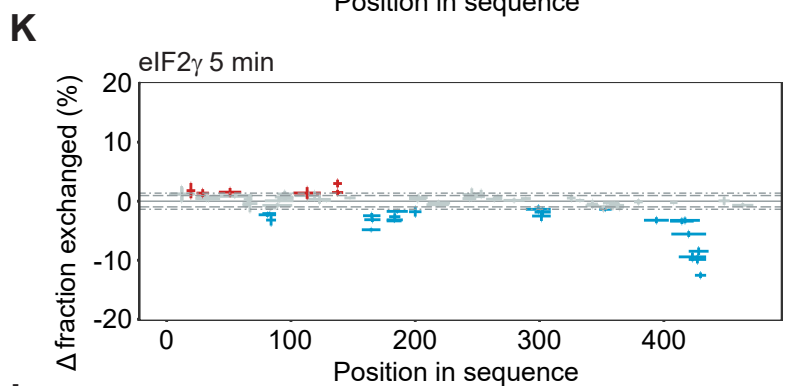
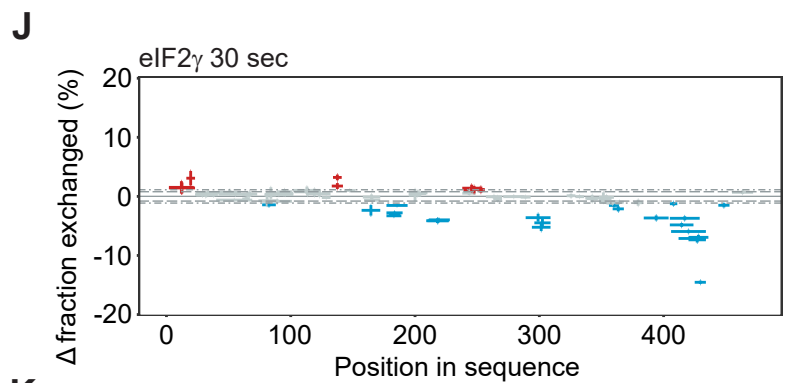
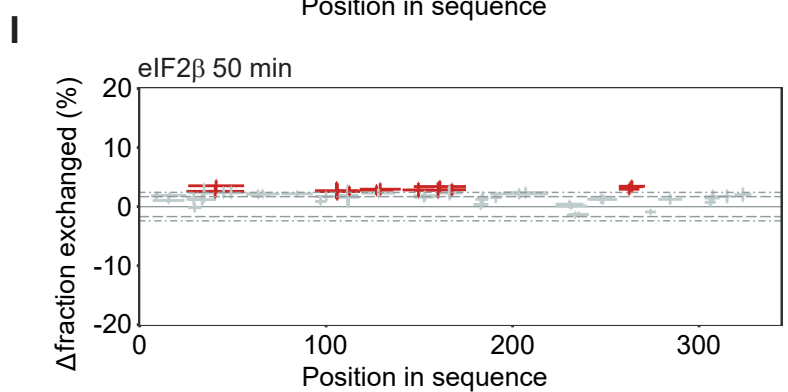
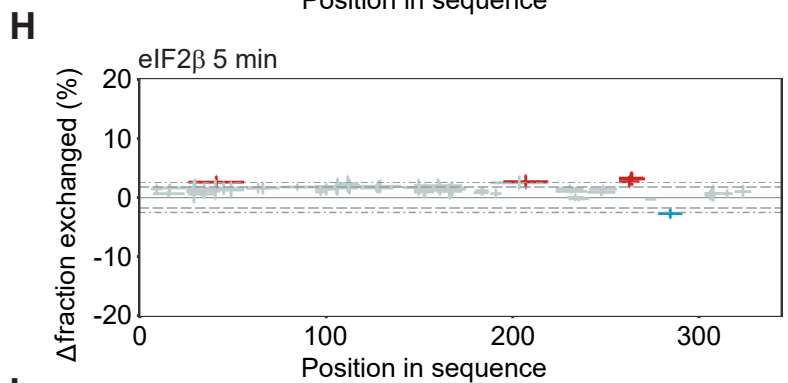
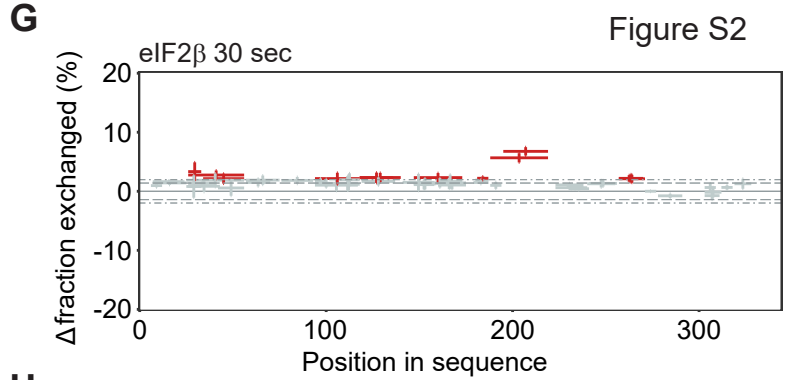
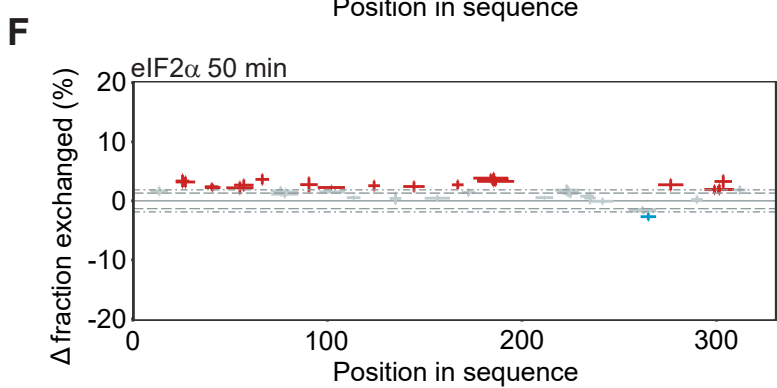
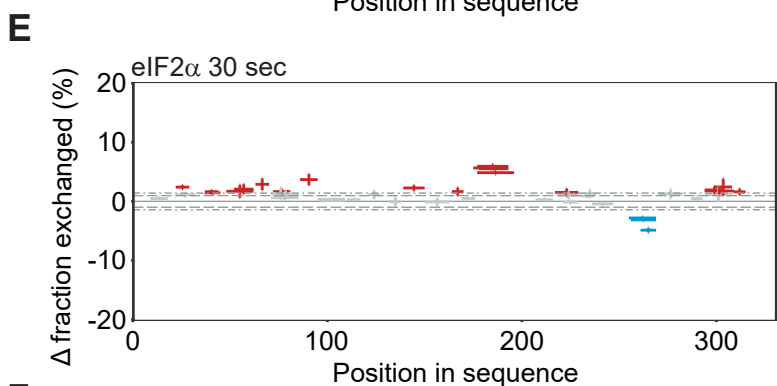
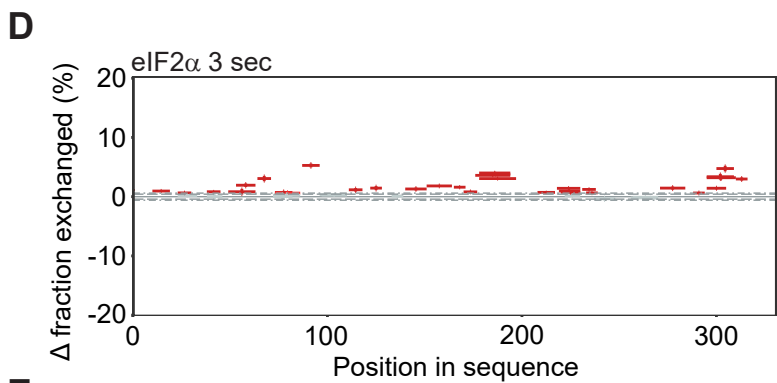
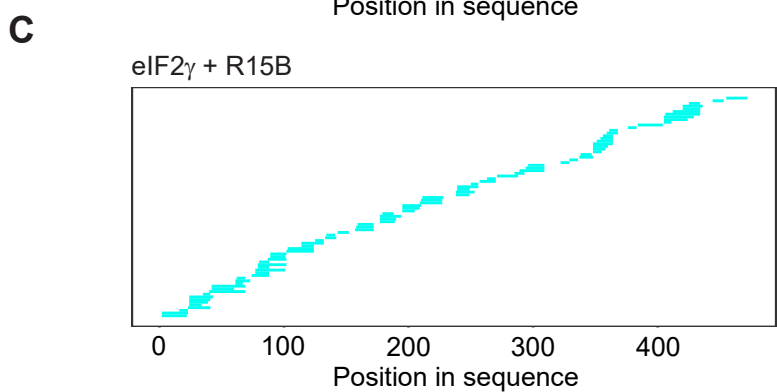
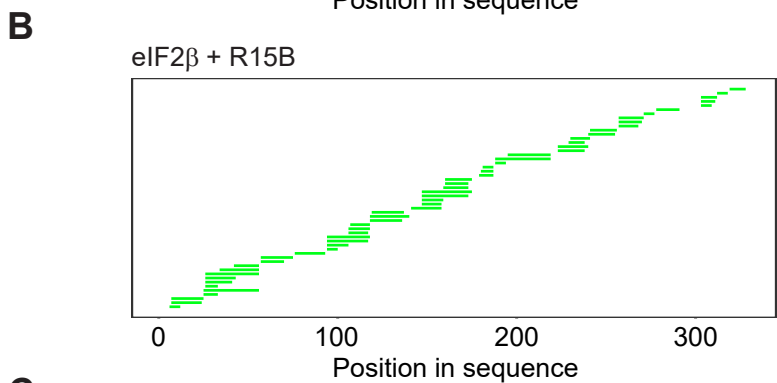
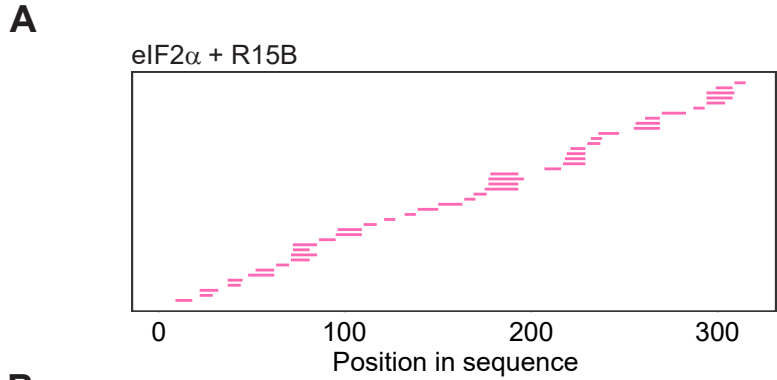
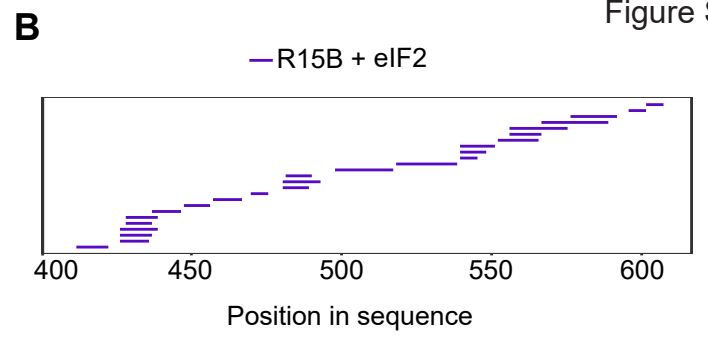
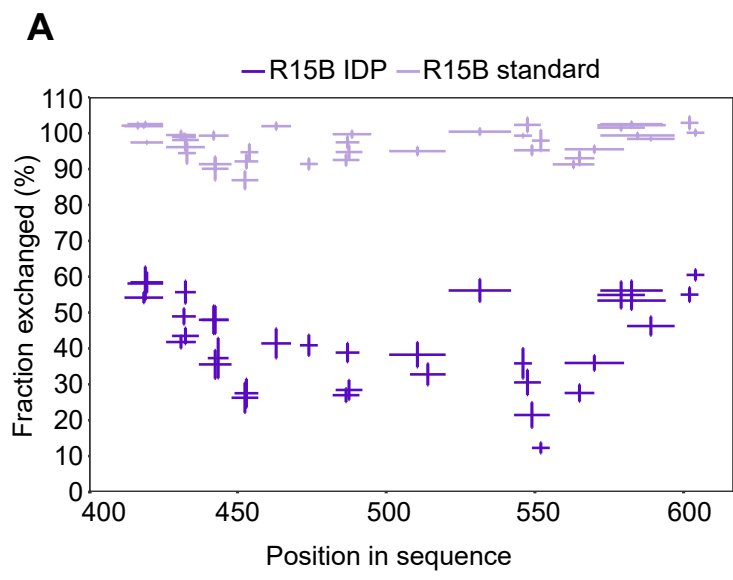


Figure S2



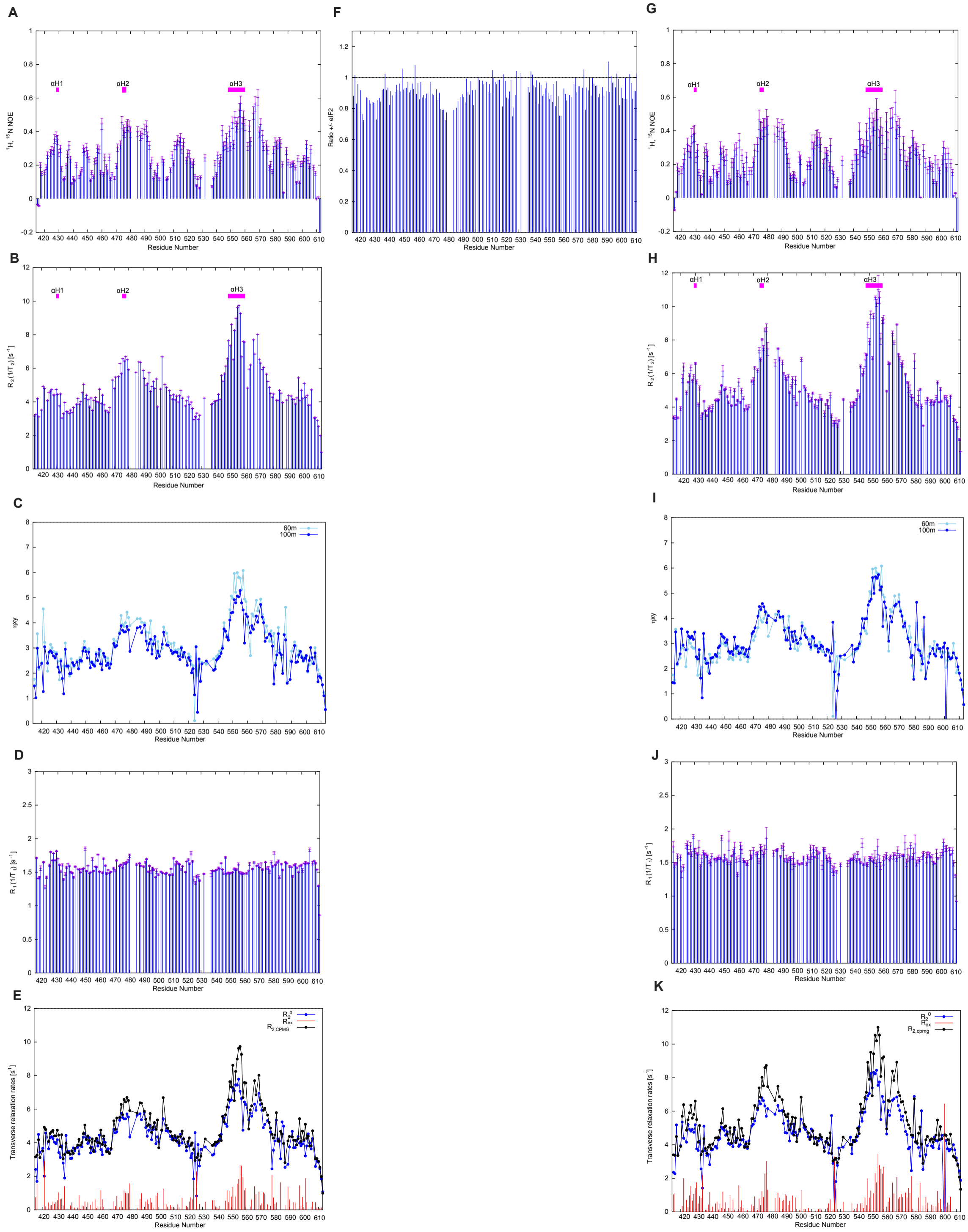
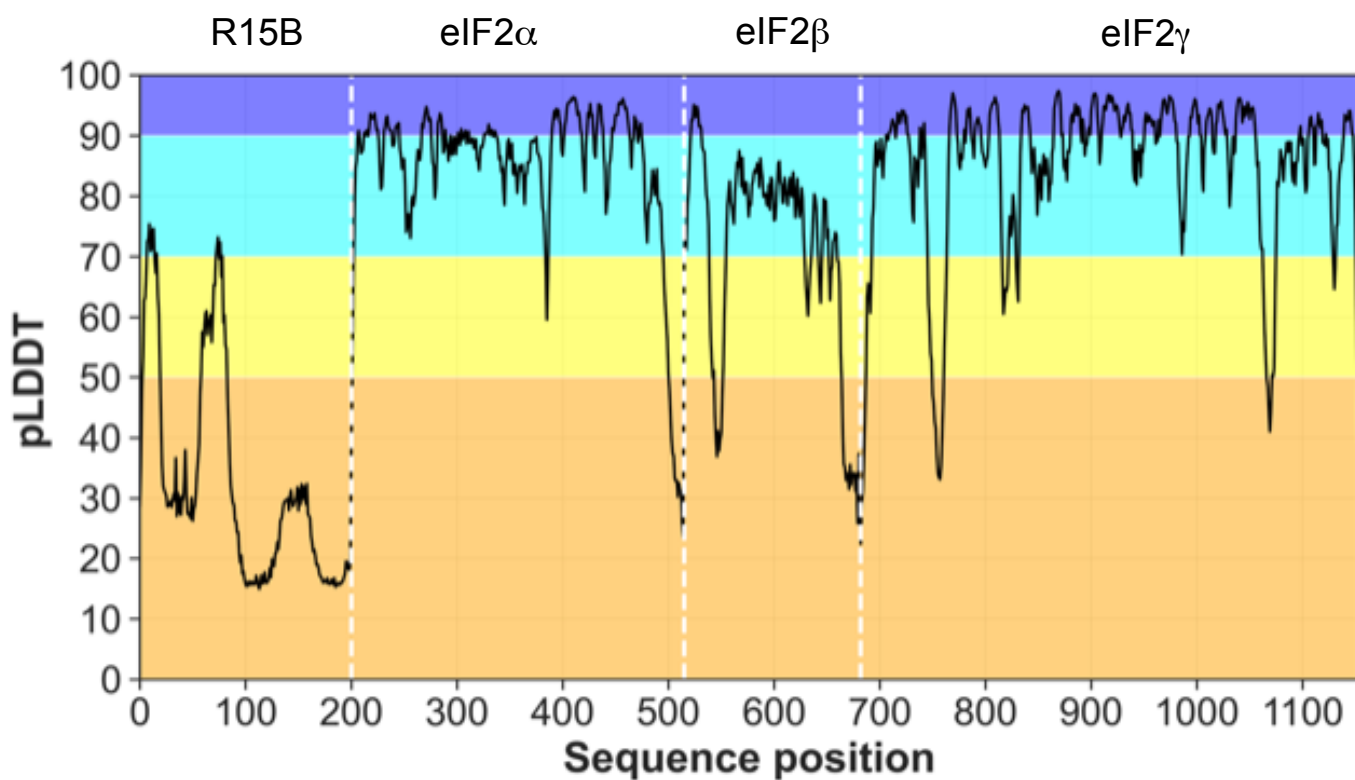




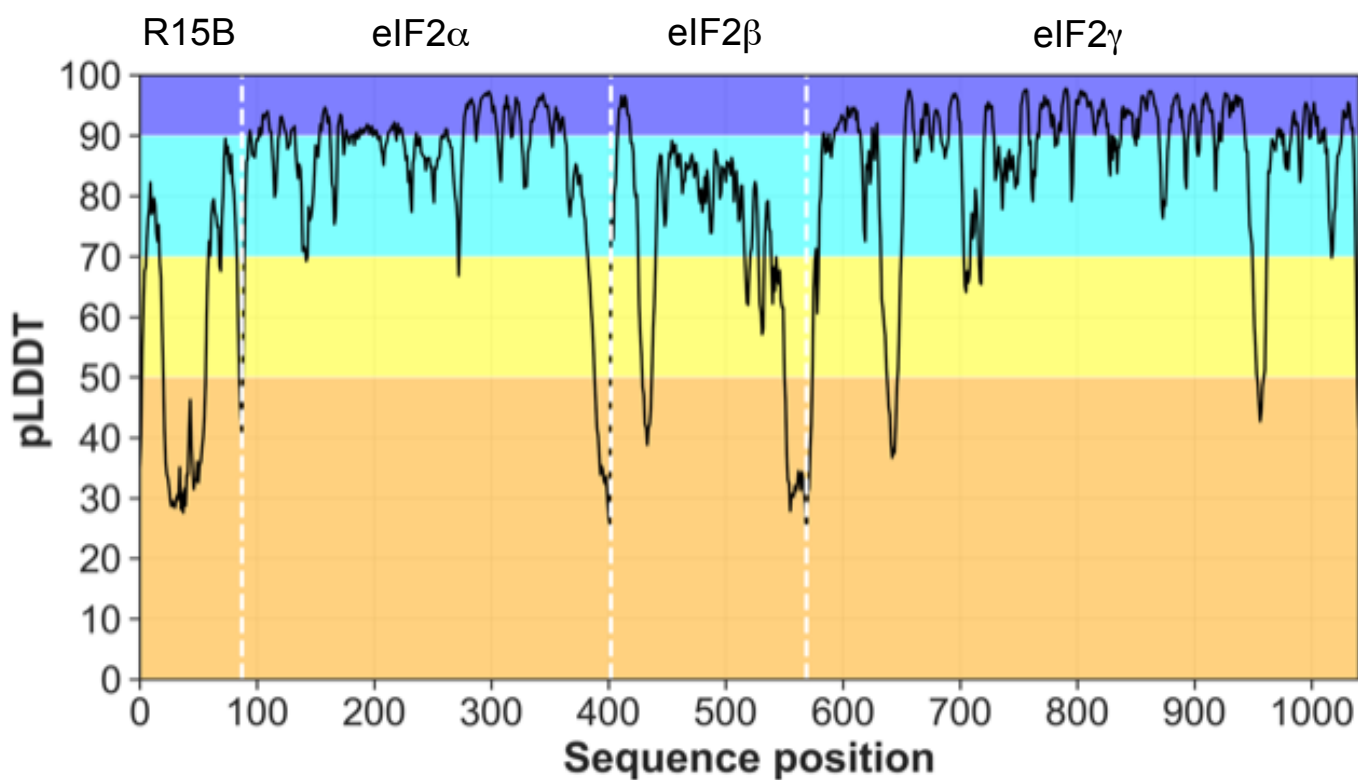


Figure S6

A



B



**Table S2 : Oligonucleotides used in this study**

<b>Primer 5'-3'</b>	<b>SOURCE</b>
R15B Forward aa1 PXJ41 ggatgacgacgataagATGGAGCCGGGGACAGGC	Sigma-Aldrich
R15B Forward aa411 PXJ41 ggatgacgacgataagGGTGACCTTCCCATTCTGCCAGAC	Sigma-Aldrich
R15B Forward aa414 PXJ41 ggatgacgacgataagCCCATTCTGCCAGACC	Sigma-Aldrich
R15B Reverse aa414 PXJ41 gtaccctcgagaactatcaGGGAAGGTCACCTTCTAGGTATGAGTAATCA	Sigma-Aldrich
R15B Reverse aa613 PXJ41 gtaccctcgagaactatcaCCCCAACAGCTGCACCTTACAAGAAAG	Sigma-Aldrich
R15B Reverse aa639 PXJ41 gtaccctcgagaactatcaTTTTCTTTGACATGTGTGTG	Sigma-Aldrich
R15B N423D site directed mutagenesis Forward AGACCAGCTTGTAGTGACAACTGATAGATTAT	Sigma-Aldrich
R15B N423D site directed mutagenesis Reverse ATAATCTATCAGTTTGTCACTACAAGCTGGTCT	Sigma-Aldrich
R15B Forward aa414 pET-47b cagggaccggtCCCATTCTGCCAGACCAGC	Sigma-Aldrich
R15B Forward aa632 pET-47b cagggaccggtAGACACACACATGTCAAAAG	Sigma-Aldrich
R15B Reverse aa613 pET-47b ggcaccagagcgtaCCCCAACAGCTGCACCTTAC	Sigma-Aldrich
R15B Reverse aa664 pET-47b ggcaccagagcgtaCCATGGTCCTTTGCGATCCTC	Sigma-Aldrich
R15B Reverse aa705 pET-47b ggcaccagagcgtaTTTGAAGCATGTTCCCTGGAGT	Sigma-Aldrich